Analysis of effective resistance calculation methods and their effect on modelling evapotranspiration in two different patches of vegetation in semi-arid SE Spain

A. Were, L. Villagarcía, F. Domingo, L. Alados-Arboledas, J. Puigdefábregas

Hydrol. Earth Syst. Sci. Discuss., 4, 243–286, 2007
www.hydrol-earth-syst-sci-discuss.net/4/243/2007/

Hydrology and Earth System Sciences Discussions

Papers published in *Hydrology and Earth System Sciences Discussions* are under open-access review for the journal *Hydrology and Earth System Sciences*

Analysis of effective resistance calculation methods and their effect on modelling evapotranspiration in two different patches of vegetation in semi-arid SE Spain

A. Were[1,2], L. Villagarcía[3], F. Domingo[2,4], L. Alados-Arboledas[1,5], and J. Puigdefábregas[2]

[1]Dept. de Física Aplicada, Univ. de Granada, 18071, Granada, Spain
[2]Estación Experimental de Zonas Áridas, Consejo Superior de Investigaciones Científicas, 04001, Almería, Spain
[3]Dept. Sistemas Físicos, Químicos y Naturales, Univ. Pablo de Olavide, 41013, Sevilla, Spain
[4]Dept. de Biología Vegetal y Ecología, Universidad de Almería, 04120, Almería, Spain

[5]Centro Andaluz de Medio Ambiente. Univ. de Granada. Junta de Andalucía, 18071, Granada, Spain

Received: 18 January 2007 – Accepted: 12 February 2007 – Published: 21 February 2007

Correspondence to: A. Were (ana@eeza.csic.es)

Abstract

Effective parameters are of major importance in modelling surface fluxes at different scales of spatial heterogeneity. Different ways to obtain these effective parameters for their use in meso-scale and GCM models have been studied. This paper deals with patch-scale heterogeneity, where effective resistances were calculated in two patches with different vegetation (*Retama sphaerocarpa* (L.) Boiss shrubs, and herbaceous plants) using different methods: aggregating soil and plant resistances in parallel, in series or by an average of both. Effective aerodynamic resistance was also calculated directly from patch fluxes. To assess the validity of the different methods used, the Penman-Monteith equation was used with effective resistances to estimate the total λE for each patch. The λE estimates found for each patch were compared to Eddy Covariance system measurements. Results showed that for effective surface resistances, parallel aggregation of soil and plant resistances led to λE estimates closer to the measured λE in both patches (differences of around 10%). This may be due to the fact that in semi-arid areas, with very sparse vegetation, soil resistances are much higher than plant resistances, and therefore parallel aggregation attenuates the effect of the high soil resistances on λE modelling. Results for effective aerodynamic resistances differed depending on the patch considered and the method used to calculate them. The use of effective aerodynamic resistance calculated from fluxes provided less accurate estimates of λE compared to the measured λE, than the use of effective aerodynamic resistances aggregated from soil and plant resistances. The results reported in this paper show that the best way of aggregating soil and plant resistances depend on the type of resistance, and the type of vegetation in the patch.

1 Introduction

Spatial heterogeneity in surface energy flux modelling, both for hydrological and meteorological purposes, is a subject of intensive research. More specifically, it is important

HESSD

4, 243–286, 2007

to study how sub-grid-scale heterogeneity can be averaged when modelling the surface fluxes in meso-scale models and GCMs.

One of the main surface fluxes is evapotranspiration, or in terms of energy, latent heat flux (λE). It can be estimated by considering that water vapour flows through a gradient of concentrations between the surface and the air, and is controlled by a set of surface and aerodynamic resistances from the different sources of evapotranspiration. Depending on the scale of heterogeneity under study, the sources of evapotranspiration that should be considered vary. In sparse-vegetation, or patch-scale heterogeneity, the plant is the roughness element that produces the surface heterogeneity. Therefore, with patch-scale heterogeneity, soil and plants are the sources of evapotranspiration considered, each with its own surface and aerodynamic resistances. At this scale, λE can be estimated using sparse-vegetation models (examples of these models are Dolman, 1993; Brenner and Incoll, 1997; Domingo et al., 1999; Verhoef and Allen, 2000). These models assume that soil and plant fluxes interact at the mean surface flow height (z_m), above which an aerodynamic resistance between this height and the reference height above the vegetation (z_r) must be taken (named the atmospheric aerodynamic resistance).

At larger scales (micro and meso-scale heterogeneity according to Mahrt, 2000), heterogeneity comes from the presence of different patches of vegetation. When modelling λE at this scale, each patch can be considered a source of λE, each with its own effective resistances (Blyth, 1995). Which brings us to the concept of the effective parameter (Fiedler and Panofsky, 1976), defined as that parameter which provides the same flux as the flux that would be calculated from contributions of individual patches, each with their own parameter (Dolman and Blyth, 1997). In this work, we used effective parameters, more specifically, patch-scale effective resistances. According to the above definition of the effective parameter, patch-scale effective resistances should provide the total patch flux.

We have calculated the effective resistances (r^e) in two patches with different vegetation, using different methods, aggregating soil and plant resistances following the

methods introduced by Blyth et al. (1993), and calculating them directly from the fluxes in the patch (Blyth, 1997; Verma, 1989). To assess the validity of the different methods used, a Penman-Monteith equation (Monteith, 1965) was used with effective resistances to estimate the total λE in each patch. The estimates of λE obtained for each patch were compared with Eddy Covariance system measurements.

2 Theory

Different methods have been developed to calculate effective resistance (r^e). Some methods are based on aggregation of local resistances, either using a probability density function (Dolman, 1992), more complex averaging schemes (McNaughton, 1994), or simple area-weighted aggregations (Blyth et al., 1993; Noilhan et al., 1997, Shuttleworth, 1997; Chehbouni et al., 2000). Other methods estimate the effective resistances at a given heterogeneous scale from the variables and fluxes measured at that scale (Blyth, 1997; Verma, 1989). In this paper we used both approaches.

2.1 Aggregation of soil and plant resistances to calculate patch-scale effective resistances

The simplest way to find the aggregated effective resistances ($\langle r^e \rangle$) at a given scale of heterogeneity is to aggregate the resistances at the smaller scale (r^i), following Ohm's Law, either in parallel:

$$\frac{1}{\langle r^e \rangle_p} = \overline{\left(\frac{1}{r^i}\right)} \tag{1}$$

or in series:

$$\langle r^e \rangle_s = \overline{r^i} \tag{2}$$

Though it is clear that surface and aerodynamic resistances from a given source must be in series (Jones, 1992), it is not clear how soil and plant resistances are related to each other. According to Blyth et al. (1993), the aggregation of resistances recommended varies depending on the flux. These authors state that for momentum, the resistances of a heterogeneous surface are set in parallel and the resulting $\langle r^e \rangle$ is weighted towards the lowest resistance. For sensible heat, the resistances are set in series and the resulting $\langle r^e \rangle$ is weighted towards the highest resistance. However, the authors find that these approximations do not always work, and that the correct $\langle r^e \rangle$ should be an average weighted by the flux. This has the disadvantage of needing to know the fluxes before calculating the effective resistances. For λE fluxes, these authors proposed a practical way to find more accurate $\langle r^e \rangle$ by averaging the resistances obtained with Eqs. (1) and (2):

$$\left\langle \overline{r^e} \right\rangle = \frac{1}{2} \left\{ \langle r^e \rangle_s + 1 \Big/ \left(\frac{1}{\langle r^e \rangle_p} \right) \right\} \tag{3}$$

This approximation has also been used by other authors to calculate $\langle r^e \rangle$ (both surface and aerodynamic) for λE (Dolman and Blyth, 1997).

Blyth et al. (1993) approximations are proposed for meso-scale and GCM models, but at patch-scale in sparsely vegetated areas, where soil and plant resistances are to be aggregated, it is not clear what kind of aggregation rules apply. Therefore, in this study, we used all three kinds of aggregation: parallel, series and an average of both (see Material and Methods section).

2.2 Calculation of patch-scale effective resistances from fluxes

The second approach for estimating r^e at a certain heterogeneous scale is to calculate it from fluxes at that scale. The equations used vary for surface and aerodynamic resistances.

Effective surface resistances (r_s^e) can be obtained from the Penman-Monteith equation (Eq. 6). Calculating r_s^e this way has the disadvantage of having to know λE first,

though it is used to model the fluxes at a higher scale when smaller scale fluxes are known (Blyth, 1997). This method was not used in our work, as we wanted to estimate patch λE with the same Penman-Monteith equation used to find the resistances.

Effective aerodynamic resistance (r_a^e), can be calculated from the patch aerodynamic parameters and friction velocity (u_*) with the equation proposed by Verma (1989) and used by other authors (Blyth, 1997; Dolman and Blyth, 1997). Assuming neutral atmospheric conditions, the aerodynamic resistance from the surface to a given reference height (z_r), can be calculated as follows:

$$r_a = \frac{u_r}{{u_*}^2} + \frac{kB^{-1}}{ku_*} \tag{4}$$

where r_a is equivalent to the patch r_a^e, u_r is the wind speed at z_r, u_* is the friction velocity and kB^{-1} is equivalent to:

$$kB^{-1} = \ln\left(\frac{z_0}{z_h}\right) \tag{5}$$

where z_0 and z_h are the roughness for momentum and sensible heat, respectively. Parameter kB^{-1} is considered constant, especially for homogeneous areas. However, $kB^{-}1$ measurements in different areas of sparse heterogeneous vegetation vary greatly, depending on surface temperature, solar radiation or on vegetation features (Kustas et al., 1989; Brutsaert, 1979; Van den Hurk and McNaughton, 1995; Qualls and Brutsaert, 1995). Different parameterizations have been made relating kB^{-1} to the Reynolds number or u_* (Mölder and Lindroth, 2001). Nevertheless, some authors have found good results for different surfaces using a kB^{-1} of approximately 2, which means that z_0 is 10 times higher than z_h (Garrat, 1978; Dolman and Blyth, 1997; Mölder and Lindroth, 2001; Verma, 1989). As explained in the Material and Methods section, we used two different values for kB^{-1}, one generic as proposed by Verma (1989), and one measured.

Calculating r_a^e this way has the advantage that soil and plant resistances need not be known in advance, thus avoiding the need for their measurement and parameterization.

2.3 Estimation of patch-scale λE with the effective resistances

As commented above, according to the definition of the effective parameter, the use of patch-scale effective resistances should provide accurate estimates of patch λE. We used a Penman-Monteith equation to estimate the patch λE, as follows:

$$\lambda E = \frac{\Delta A + \left(\rho c_p D_a / r_a^e\right)}{\Delta + \gamma\left(1 + r_s^e / r_a^e\right)} \quad (6)$$

where A is the available energy, ρ is the air water vapour density at z_r, c_p is the specific heat of air, Δ is the slope of the curve relating saturated air water vapour pressure to temperature, γ is the psychrometric constant and D_a is the water vapour pressure deficit at z_r. r_s^e and r_a^e are the effective surface and aerodynamic resistances of each patch, calculated with the different methods described in the Material and Methods section as mentioned above.

3 Material and methods

Field experiments for measuring the aerodynamic and surface resistances of soil and plants, and the different micro-meteorological variables and λE, were carried out in two patches of sparse semi-arid vegetation characteristic of southeastern Spain.

3.1 Site description

The field site is located in Rambla Honda, a dry valley near Tabernas, Almería, Spain (37° 8′ N, 2°22′ W, 630 m altitude). The field site has previously been described in detail elsewhere (see e.g., Puigdefábregas et al., 1996, 1998, 1999; Domingo et al., 1999, 2001). The valley bottom is a dry river bed with deep loamy soils that overlay mica-schist bedrock, dominated by *Retama sphaerocarpa* (L.) Boiss shrubs separated by bare areas dominated by herbaceous species.

The field site has an average annual rainfall of 220 mm, average mean temperature of 16°C and a dry season from around June to September.

The patches selected were located on the east bank of the dry river bed on the valley floor. A 100 m^2 patch was selected in which all the *R. sphaerocarpa* was cut, leaving a patch with only the herbaceous stratum (Fig. 1).

R. sphaerocarpa is a woody leguminous shrub with ephemeral leaves and cylindrical photosynthetic stems (cladodes), which grows up to 4 m tall and 6 m diameter. It has an open canopy structure and deep root system which can extract water from depths of more than 25 m (Domingo et al., 1999; Domingo et al., 2001; Haase et al., 1996). Growth starts in March, flowering is in May, and fructification is from July to September. New shoots germinate in January and February. The average fractional vegetative cover (f) of the *R. sphaerocarpa* patch was 0.17, and the average leaf area index (L) of the *R. sphaerocarpa* plants was 0.81 $m^2\,m^{-2}$.

The herbaceous species are predominantly annuals or therophytes, with few hemicryptophytes or cryptophytes (Gutiérrez, 2000). Biomass is picked in spring, between March and May, though this varies in different years. The growing period starts in October or November, after the first rains, and continues until March or April. Flowering is from February to April, and fructification from March to May. During the summer there are practically no herbaceous plants. Herbaceous phenology is very sensitive to precipitation in fall and spring, so the periods of growth, flowering, fructification and senescence may vary in different years (Gutiérrez, 2000), and is also the reason why the average f of the herbaceous patch varied during the experiment.

3.2 Measurement and parameterization of soil and plant resistances

Several field experiments were performed to measure and parameterize the soil and plant resistances in the two patches.

As shown in Fig. 2a, in the *R. sphaerocarpa* patch, the surface resistances considered were for plant (r_s^p), soil under plant (r_s^{su}) and bare soil (r_s^{bs}), and their respective aerodynamic resistances (r_a^p, r_a^{su} and r_a^{bs}). As mentioned in the Introduction, an aero-

dynamic resistance between the mean flow height ($z_m = z_0 + d$) and the reference height (z_r), referred to here as the atmospheric aerodynamic resistance (r_a^a), was also considered. In the herbaceous patch (Fig. 2b), only one soil surface resistance and one soil aerodynamic resistance were considered (r_s^s and r_a^s, respectively), as any difference between soil under plant and bare soil was neglected. The rest of the resistances were the same as in the other patch. r_s^s, r_s^{su} and r_s^{bs} were measured with microlysimeters following the methodology proposed by Daamen et al. (1993). The values measured were related to soil moisture (θ) from which different parametric equations were obtained (see Table 1). This method has also been used successfully by Domingo et al. (1999) in the Rambla Honda field site to estimate soil surface resistances in another patch of *R. sphaerocarpa* close to the one described in this paper.

Soil aerodynamic resistances were measured using the energy balance of heated sensors method developed by McInnes et al. (1994, 1996). In the herbaceous patch, measured r_a^s was related to wind speed at z_r (u_r), to find a parametric equation for it (Table 1). In the *R. sphaerocarpa* patch, the parametric equations relating r_a^{su} and r_a^{bs} to u_r were those obtained by Domingo et al. (1999) using the same methodology (Table 1).

Plant resistance r_s^p was calculated from its opposite, plant conductance (g_s^p), which is related to leaf conductance (g_s^l) as follows :

$$1/r_s^p = g_s^p = 2g_s^l L \quad (7)$$

g_s^l measurements in different plants in the herbaceous patch were taken with a porometer with an IRGA (LCA-3, ADC, Hoddesdon, UK) and a PLC-3 chamber (ADC, Hoddeson, UK). The averaged values were related to D_a obtaining the parametric equation used for the herbaceous patch (Table 2).

The parametric equations used for *R. sphaerocarpa* relating this conductance to photosynthetically active radiation flux (Q), D_a and θ were those found by Brenner and Incoll (1997) at the same site. According to Baldocchi et al. (1991) g_s^l can be calculated

as:

$$g_s^l = g_s^m Q / (Q + b_q) \quad (8)$$

where g_s^m is the maximum g_s^l at light saturation dependent on D_a:

$$g_s^m = g_s^{\max} + b_d D_a \quad (9)$$

Brenner and Incoll (1997) related the daily average of the measured conductance to D_a on different days, and $g_s^{\max}$ (maximum g_s^l at light saturation and air water vapour saturation) and b_d (indicator of g_s^l changes with D_a) were related to θ (see equations in Table 2).

Once g_s^m is known, and considering that Q decreases through the canopy by the coefficient of extinction of the canopy (κ), g_s^p is calculated as (Shuttleworth and Gurney, 1990):

$$g_s^p = (g_s^m / \kappa) \ln \left[(b_q + \kappa Q) / \left(b_q + \kappa Q e^{\kappa L} \right) \right] \quad (10)$$

where b_q is the coefficient of linearity between the values of g_s^l measured and estimated with Eq. (8) (b_q=200 mol m^{-2} s^{-1}). r_a^p was calculated following the equations proposed by Shuttleworth and Wallace (1985) and Choudhoury and Monteith (1988). Similar to Eq. (7):

$$r_a^p = r_a^l / 2L \quad (11)$$

where r_a^l is the average leaf aerodynamic resistance of the canopy leaves, calculated as:

$$r_a^l = (n/a) (w/u_h)^{0.5} \left(1 - e^{(-n/2)} \right)^{-1} \quad (12)$$

where a is a constant that relates r_a^l with u_h (Domingo et al., 1996), w is the average width of the leaves and u_h is the wind speed above vegetation, calculated as:

$$u_h = \left(u_* / k \right) \ln \left[(h - d) / z_0 \right] \quad (13)$$

where h is the height of vegetation, d is the displacement height, z_0 is the roughness, k is the von Karman constant, and u_* is the friction velocity calculated as:

$$u_* = k u_r / \ln\left[(z_r - d)/z_0\right] \quad (14)$$

r_a^a was also calculated with theoretical equations developed by Shuttleworth and Gurney (1990). In the end, r_a^a is calculated as:

$$r_a^a = \left(1/k u_*\right) \ln\left[(z_r - d)/(h - d)\right](1 + \delta)^{\varepsilon} + \left(h/nK_h\right)\left[e^{\{n[1-(z_o+d)/h]\}} - 1\right] \quad (15)$$

where K_h is the turbulent diffusion coefficient for water vapour above the vegetation, n is the coefficient indicating the decrease in the turbulent diffusion through the vegetation, and $(1 + \delta)^{\varepsilon}$ is a correction factor for the stability atmospheric conditions. z_0 and d were calculated with the equations used by Shuttleworth and Gurney (1990) relating these parameters to the L_p (patch leaf area index = L/f) and h.

Table 3 shows the values of the vegetation parameters needed to calculate these resistances. L and f in the herbaceous patch were estimated from biomass measurements. f ranged from 0 (near summer) to 0.4 (in spring), depending on the phenology of the plants in the patch. An equation relating L to f was obtained: $L = 5.8 f^{0.78}$ (R^2=0.99, n=8). In the *R. sphaerocarpa* patch, L was measured in individual *R. sphaerocarpa* plants with a Sunscan system (Delta Devices Ltd., Cambridge, UK) and averaged. f was calculated from measurements of the projected plant canopy area in selected stands in the patch.

3.3 Calculating the effective resistances (r^e) for each patch

As mentioned above in the Theory section, one of the methods used to calculate the surface and aerodynamic effective resistances for each patch, r_s^e and r_a^e (Fig. 2), was to aggregate soil and plant resistances, thus obtaining the effective aggregated surface and aerodynamic resistances, $\langle r_s^e \rangle$ and $\langle r_a^e \rangle$.

In the case of $\langle r_a^e \rangle$, we aggregated the aerodynamic resistances of soil and plant, and also the atmospheric aerodynamic resistance, as $\langle r_a^e \rangle$ represents the total aerodynamic resistance from soil to reference height (z_r) (Fig. 2). Therefore $\langle r_a^e \rangle$ was calculated aggregating soil and plant aerodynamic resistances, weighted by f, either in series or in parallel, while r_a^a was always aggregated in series as this is its position relative to the other aerodynamic resistances (Fig. 2). Therefore the equations for the *R. sphaerocarpa* patch were:

$$\langle r_a^e \rangle_p = \left(f \left(\frac{1}{r_a^p} + \frac{1}{r_a^{su}} \right) + (1-f) \left(\frac{1}{r_a^{bs}} \right) \right)^{-1} + r_a^a \tag{16}$$

$$\langle r_a^e \rangle_s = f \left(r_a^p + r_a^s \right) + (1-f)\, r_a^{bs} + r_a^a \tag{17}$$

and for the herbaceous patch:

$$\langle r_a^e \rangle_p = \left(f \left(\frac{1}{r_a^p} \right) + (1-f) \left(\frac{1}{r_a^s} \right) \right)^{-1} + r_a^a \tag{18}$$

$$\langle r_a^e \rangle_s = f r_a^p + (1-f)\, r_a^s + r_a^a \tag{19}$$

In the case of $\langle r_s^e \rangle$, we also aggregated the surface soil and plant resistances, weighed by f, either in parallel or in series. The equations for the *R. sphaerocarpa* patch were:

$$\frac{1}{\langle r_s^e \rangle_p} = f \left(\frac{1}{r_s^p} + \frac{1}{r_s^{su}} \right) + (1-f) \left(\frac{1}{r_s^{bs}} \right) \tag{20}$$

$$\langle r_s^e \rangle_s = f \left(r_s^p + r_s^s \right) + (1-f)\, r_s^{bs} \tag{21}$$

and for the herbaceous patch:

$$\frac{1}{\langle r_s^e \rangle_p} = f \left(\frac{1}{r_s^p} \right) + (1-f) \left(\frac{1}{r_s^s} \right) \tag{22}$$

$$\langle r_s^e \rangle_s = f r_s^p + (1 - f) r_s^s \quad (23)$$

In all equations $\langle r^e \rangle_s$ and $\langle r^e \rangle_p$ refer to effective resistances aggregated in series and in parallel, respectively.

We also averaged the effective resistances aggregated in parallel and in series (Eq. 3) to find the average aggregated effective surface and aerodynamic resistances, $\left\langle \overline{r_s^e} \right\rangle$ and $\left\langle \overline{r_a^e} \right\rangle$, for each patch.

The other calculation method, mentioned above in the Theory section, was only used in this paper for the effective aerodynamic resistance (r_a^e) (Eq. 4). Two different values of kB^{-1} were used to calculate r_a^e for each patch: i) 2.3 as proposed by Verma (1989) and used by some authors for heterogeneous surfaces (Blyth, 1997; Dolman and Blyth, 1997), the resulting resistance being referred to as $r_{a_1}^e$; ii) the average of 9 (SD = 6) obtained by Alados-Arboledas et al. (2000) from radiometric temperature measurements in a patch of *R. sphaerocarpa* in the Rambla Honda field site, the resulting resistance then being referred to as $r_{a_2}^e$. u_* was calculated using Eq. (14).

3.4 Micrometeorological and energy flux measurements

Latent (λE) and sensible (H) heat fluxes were measured by an Eddy covariance station in a tower at the reference height in the northern part of each patch, where due to the dominant wind direction, they have the best fetch (Fig. 1). The Eddy covariance systems consisted of a three-dimensional sonic anemometer (CSAT3, Campbell Scientific Inc., USA) and a krypton hygrometer KH20 (CSAT3, Campbell Scientific Inc., USA). λE measurements were corrected for air density fluctuation due to heat and water vapour flux as proposed by Webb et al. (1980). Hygrometer measurements were corrected for absorption of radiation by oxygen, according to Tanner et al. (1993). The rotation of the coordinate system (Kowalski et al., 1997) was unnecessary, because as the terrain is near a river bed, it is almost flat, and it was verified that the values barely change with this correction.

The wind speed and air temperature at reference height (u_r and T_r) were measured with the sonic anemometer. The water vapour pressure at reference height (e_r) required for calculation of D_a was measured with a dew point hygrometer (Dew-10, General Eastern Corp., USA). R_n was measured with a radiometer (NR Lite, Kipp and Zonen, Delft, the Netherlands).

Patch soil heat flux (G) was calculated as the sum of the flux measured with two soil heat flux plates (HFT-3, REBS, Seattle, WA, USA) at a depth of 0.08 m (F) in each patch, and the heat stored in the layer of soil above the plates (S_t) (Fuchs, 1986; Massman, 1992):

$$S_t = \Delta T_s \left[B_d(C_s + C_w\theta)\right] Dp/t \quad (24)$$

where B_d is the apparent density of soil (1555 kg m^{-3} according to Puigdefábregas et al., 1996), C_s is the specific heat of dry soil, C_w is the specific heat of water, Dp is the depth at which the soil heat flux plate is located, t is the time lapse between measurements, and ΔT_s is the changing rate of soil temperature between two consecutive measurements by two thermocouples (TCAV, Campbell Scientific Ltd.) at two depths (0.02 m and 0.06 m) above each soil heat flux plate.

Soil moisture (θ) was measured with 6 self-balanced impedance bridge (SBIB) probes in the herbaceous patch, and 12 in the *R. sphaerocarpa* patch in a range of positions from soil under plant to bare soil at a depth of 0.04 m. This soil humidity sensor developed by the Estación Experimental de Zonas Áridas (C.S.I.C., Almería, Spain) (Vidal, 1994; Vidal et al., 1996) has been used in other work (see e.g., Puigdefábregas and Sanchez, 1996; Domingo et al., 2000; Canton et al., 2004).

All of the micrometeorological variables and heat fluxes (λE, H, R_n, F, u_r, T_r, e_r, θ and T_s) measurements were averaged every 30 min and recorded in dataloggers (Campbell Scientific Ltd., Logan, UT, USA) from April 2002 (DOY 91) to July 2003 (DOY 198).

3.5 Data set used

All measured data were filtered using the following criteria. In the first place, days lacking data for any of the energy fluxes necessary to analyse the energy balance (i.e., R_n, G, λE and H) were eliminated. Data with a negative R_n were also eliminated, leaving only the data for daylight hours (from 8:00 to 16:00 h), because heat fluxes at night are erratic and difficult to predict. Rainy-day data was eliminated, as condensation forms on the krypton hygrometer, making λE data unreliable. The final dataset selected included daytime λE high enough to be reliable and excluded data with λE near 0 W m^2, which is typical of cloudy days and during the dry season. The result was a dataset for micrometeorological variables and energy fluxes on discontinuous days between DOY 52 and 71 (11 days for the *R. sphaerocarpa* patch, and 13 days for the herbaceous patch).

To assess the accuracy of measured λE, the energy balance of the fluxes was analysed with a regression between the measured available energy (R_n–G) and the sum of the turbulent fluxes (λE + H) for the period studied (Fig. 3). The data showed an acceptable energy balance closure of nearly 90% (b=0.88, R^2=0.89 for the *R. sphaerocarpa* patch, and b=0.89, R^2 = 0.86 for the herbaceous patch).

4 Results and discussion

4.1 Comparison of effective resistances calculated for each patch

To compare the effective resistances calculated, the average percentage difference between them (Δr) was found by:

$$\Delta r\,(\%) = \overline{\left(\frac{(r_i - r_j)}{r_i}\right)} * 100 \qquad (25)$$

where r_i and r_j are the resistances compared, and r_j is a percentage X higher (negative) or lower (positive) than r_i. Table 4 shows the average Δr for each patch.

When the effective aerodynamic resistance was compared, the differences between the resistances calculated with Eq. (4) were around 50% in both patches, with $r^e_{a_2}$ higher than $r^e_{a_1}$. When these were compared with the aggregated resistances, $\langle r^e_a \rangle_p$ was around 50% lower than $r^e_{a_1}$ and around 75% lower than $r^e_{a_2}$ in both patches. However, the differences between $r^e_{a_1}$, and $\langle r^e_a \rangle_s$ and $\left\langle \overline{r^e_a} \right\rangle$ are not significant, as the SD is very high. $\langle r^e_a \rangle_s$ was around 40% lower and $\left\langle \overline{r^e_a} \right\rangle$ was around 60% lower than $r^e_{a_2}$ in both patches. For a better analysis of these differences, the effective aerodynamic resistances were plotted against u_r (Fig. 4), since the soil, plant and atmospheric aerodynamic resistances depend on this variable, as well as $r^e_{a_1}$ and $r^e_{a_2}$. This figure showed that the differences between $r^e_{a_1}$, and $\langle r^e_a \rangle_s$ and $\left\langle \overline{r^e_a} \right\rangle$ changed with u_r. At high u_r ($>2\,\mathrm{m\,s^{-1}}$) the values of $r^e_{a_1}$ were similar to $\left\langle \overline{r^e_a} \right\rangle$ and lower than $\langle r^e_a \rangle_s$. As u_r got lower, $r^e_{a_1}$ got higher than $\langle r^e_a \rangle_s$ and $\left\langle \overline{r^e_a} \right\rangle$ (Fig. 4). These results show that $r^e_{a_1}$ and $r^e_{a_2}$ were much more sensitive to u_r than the aggregated resistances, as the latter also depend on the vegetation parameters (L, h and f) and on the temperature.

When comparing the aggregated resistances, it was observed that $\langle r^e_a \rangle_p$ was around 50% and 60% lower than $\langle r^e_a \rangle_s$, for the *R. sphaerocarpa* and the herbaceous patch, respectively (Table 4).

When the surface resistances were compared, though $\langle r^e_s \rangle_p$ was lower than $\langle r^e_s \rangle_s$, as was the case with the aerodynamic resistances, there was much less difference between them in the *R. sphaerocarpa* patch (around 40%) than in the herbaceous patch (around 80%) (Table 4). This can be observed in Fig. 5, where the aggregated surface resistances were plotted against soil moisture (θ), which soil and plant surface resistances depend on.

In the herbaceous patch, $\langle r_s^e \rangle_p$ was observed to be much lower than $\langle r_s^e \rangle_s$ and less dependent on θ, while $\langle r_s^e \rangle_s$ varied considerably with θ and covered a wide range of values (hence the high SD in Table 4). In the *R. sphaerocarpa* patch, $\langle r_s^e \rangle_p$ and $\langle r_s^e \rangle_s$ were much closer and varied similarly with θ.

To understand the differences in aggregated resistances between the two patches, and between surface and aerodynamic resistances, we compared them to the soil and plant resistances (and to the atmospheric aerodynamic resistance, in the case of $\langle r_a^e \rangle$) in each patch (Figs. 6 and 7).

As seen in Fig. 6, the soil, plant and atmospheric aerodynamic resistances were similar in both patches. The effect of r_a^p on $\langle r_a^e \rangle_p$ was stronger in the herbaceous patch, because in the *R. sphaerocarpa* patch r_a^{su} diminished the effect of r_a^p (according to Eq. 16).

With regard to surface resistances, soil resistances were much higher than plant resistances in the herbaceous patch (Fig. 7). Therefore, in the herbaceous patch, the effect of aggregating resistances in parallel or in series generated wide differences in the effective resistances found, even though f was less than 0.2. However, in the *R. sphaerocarpa* patch, there was not as much difference between soil and plant resistances (Fig. 7), and f was low (0.17), so the effect of how aggregation was done on the effective surface resistance was not as great in this patch.

Regardless of the type of effective resistance, in all cases aerodynamic resistances were many times lower than surface resistances, and therefore their effect on the estimation of λE was also slight, as previously reported by other authors (Verhoef and Allen, 1998).

4.2 Comparing λE estimated using the effective resistances and λE measured in each patch

λE estimated with Eq. 6 was compared to λE measured in each patch. λE was estimated using the aggregated surface resistances ($\langle r_s^e \rangle_p$,$\langle r_s^e \rangle_s$ and $\left\langle \overline{r_s^e} \right\rangle$) combined

with the effective aerodynamic resistances calculated with Eq. 4, r^e_{a1} and r^e_{a2}, (Fig. 8, Table 5), and the aggregated aerodynamic resistances, $\langle r^e_a \rangle_p$,$\langle r^e_a \rangle_s$ and $\left\langle \overline{r^e_a} \right\rangle$ (Fig. 9, Table 6).

First of all, when the results found for each patch were compared, the estimates found using different $\langle r^e_s \rangle$ in the *R. sphaerocarpa* patch were observed to be similar (Fig. 8a1 and a2 and Fig. 9a1 and a2). Estimated average daily λE ranged from 0.9 mm day^{-1} using $\langle r^e_s \rangle_p$ with r^e_{a2} to 0.49 mm day^{-1} using $\langle r^e_s \rangle_s$ with r^e_{a1}; and from 0.77 mm day^{-1} using $\langle r^e_s \rangle_p$ with $\langle r^e_a \rangle_s$, to 0.36 mm day^{-1} using $\langle r^e_s \rangle_s$ with $\langle r^e_a \rangle_p$. However, in the herbaceous patch, there was clearly a wide difference between λE estimated with $\langle r^e_s \rangle_p$and with $\langle r^e_s \rangle_s$ or $\left\langle \overline{r^e_s} \right\rangle$, regardless of the aerodynamic effective resistances used (Fig. 8b1 and b2 and Fig. 9b1 and b2). Estimated average daily λE ranged from 1.01 mm day^{-1} using $\langle r^e_s \rangle_p$ with r^e_{a2}, to 0.26 mm day^{-1} using $\langle r^e_s \rangle_s$ with r^e_{a1}; and from 0.88 mm day^{-1} using $\langle r^e_s \rangle_p$ with $\langle r^e_a \rangle_s$, to 0.18 mm day^{-1} using $\langle r^e_s \rangle_s$ with $\langle r^e_a \rangle_p$.

When the estimated and measured λE were compared, results in the *R. sphaerocarpa* patch showed that when the aggregated effective resistances were used, the combination of $\langle r^e_s \rangle_p$ and $\langle r^e_a \rangle_s$ provided λE estimates closer to the measured values (Table 6 and Fig. 9). When aerodynamic resistances r^e_{a1} and r^e_{a2} were used, the results were not so clear. Using r^e_{a2}, calculated with measured kB^{-1}, λE was closer to the measured λE, particularly with $\langle r^e_s \rangle_p$ (Table 5). However, the combination of r^e_{a1}, calculated with a generic kB^{-1}, with $\langle r^e_s \rangle_p$ also generated λE estimates similar to the measured values (Table 5).

In the herbaceous patch, results showed that when using aerodynamic resistances r^e_{a1} and r^e_{a2}, the regressions between measured values and estimates using r^e_{a1} were very close, with b from 0.7 to 0.96, and R^2 from 0.48 to 0.67 (Table 5). With these results, we found that λE estimated using $\langle r^e_s \rangle_p$ was higher than measured λE, while λE estimated with $\langle r^e_s \rangle_s$ and $\left\langle \overline{r^e_s} \right\rangle$ was lower (Fig. 8). When using aggregated aerody-

namic resistances, the regressions between measured and estimated λE had a lower b and R^2 than those found with r^e_{a1} and r^e_{a2}. b ranged from 0.29 to 0.76, and R^2 from 0.36 to 0.6. However, it seemed that the estimates found with $\langle r^e_s \rangle_p$ were closer to the measured values, as was the case in the *R. sphaerocarpa* patch.

The results of the regressions made between measured and estimated λE were not conclusive, especially in the herbaceous patch, which had a very high intercept a. We therefore averaged the differences between the measured and estimated values, $\Delta\lambda E$, calculated with an equation equivalent to Eq. (25), substituting r_i and r_j with the daily measured λE and estimated λE, respectively. Results are shown on Tables 7 and 8.

In the *R. sphaerocarpa* patch, effective resistances $\langle r^e_s \rangle_p$ and $\langle r^e_a \rangle_s$ generated better estimates of λE compared to the measured values, with a $\Delta\lambda E$ of less than 10% (Table 8), which is within the energy balance closure of the measured data. However, when using r^e_{a2} combined with $\langle r^e_s \rangle_p$ or even with $\left\langle \overline{r^e_s} \right\rangle$, λE estimates differed by only 13% (absolute values) from the measured λE (Table 7). Using r^e_{a1} again combined with $\langle r^e_s \rangle_p$, the estimated λE was fairly close to measured λE, with a 15% difference (absolute values). Therefore, these results showed that the surface resistances that led to the best estimates of λE were $\langle r^e_s \rangle_p$, and the aerodynamic resistances were $\langle r^e_a \rangle_s$ and r^e_{a2}.

In the herbaceous patch, regardless of the effective aerodynamic resistances used, $\langle r^e_s \rangle_p$ were the effective surface resistances that provided the best estimates of λE compared to measured values, as was also the case in the *R. sphaerocarpa* patch. The combinations of $\langle r^e_s \rangle_p$ with $\langle r^e_a \rangle_p$ and $\left\langle \overline{r^e_a} \right\rangle$ generated the λE estimates closest to the measured λE, with average differences of 13% and 15%, respectively (Table 8). When aerodynamic resistances calculated with Eq. (4) were used, the λE estimates differed widely from the measured λE, with differences of from 21% when using r^e_{a1} with $\langle r^e_s \rangle_p$, to 65% when using $\langle r^e_s \rangle_s$ with r^e_{a2} (Table 7). As r^e_{a2} is calculated with a kB^{-1} measured in a patch of *R. sphaerocarpa,* this resistance would not be expected to be

suitable for a patch of herbaceous plants, with very different aerodynamic parameters.

It may be observed that the SDs of the means of $\Delta\lambda E$ were very high, showing wide dispersion of the results. This was because we used measured values of λE as well as the variables and parameters used in its estimation. Considering that the use of effective parameters involved a simplification of the spatial heterogeneity in the patches, an error in the estimations was expected. However, as the use of effective parameters and the aggregation of spatial heterogeneity are necessary to model the fluxes at higher scales of heterogeneity, the results reported in this paper are important because they show the effect of these effective parameters at patch-scale and using measured values.

The overall results show that the type of effective surface resistances used is what most affected the λE estimates. Thus in both patches, the surface resistances aggregated in parallel gave the best estimates of λE. This suggests that this type of aggregation is the most suitable for estimating patch-scale effective surface resistances, which does not coincide with the idea that the average of resistances aggregated in series and in parallel ($\left\langle \overline{r^e} \right\rangle$), as proposed by Blyth et al. (1993), would generate the best estimates of λE. It should be noted that to estimate λE, these authors used the aggregation of theoretical resistances in two patches, while we analysed the aggregation of measured soil and plant resistances. Moreover, the best estimates of λE obtained with parallel aggregation of surface resistances, may be due to the fact that soil resistances are higher than plant resistances, and the vegetative cover fraction is very small, which is characteristic of semi-arid areas. Parallel aggregation of the resistances attenuated the effect of the high soil resistances.

Results for aerodynamic resistances were not the same in the two patches. While in the *R. sphaerocarpa* patch the effective aerodynamic resistances aggregated in series produced the best estimates of λE, in the herbaceous patch the effective aerodynamic resistances aggregated in parallel, or even the average of resistances aggregated in parallel and in series, gave acceptable results. Other authors, like Chehbouni et al. (1997) and Chehbouni et al. (2000) have aggregated resistances in parallel in

two patches of different types of vegetation to estimate the aggregated effective aerodynamic resistance for sensible heat.

These results show that, again the most suitable aggregation method for estimating effective resistances changes depending on the type of resistance, on the scale of heterogeneity and on the type of vegetation.

The regressions between estimated and measured λE were better with the effective aerodynamic resistances calculated directly from wind speed and kB^{-1} than with aggregated resistances in both patches, though when the differences are analysed in %, the differences are greater with the effective aerodynamic resistances calculated from wind speed and kB^{-1}. However, when using a kB^{-1} measured in an *R. sphaerocarpa* patch, the λE estimates in a nearby patch were quite similar to the measured λE (differences of around 13%). Using a generic kB^{-1}, used by other authors in other patches of vegetation (Blyth, 1997), estimates of λE had an error of around 20% compared to the measurements in both patches. This method of estimating the effective aerodynamic resistances for the patch has the advantage of not requiring complex measurements or parameterizations, though there is a wider error than with aggregated soil and plant aerodynamic resistances.

5 Conclusions

- In a semi-arid area, where surface resistances are very high, the patch-scale effective surface resistance affects the estimation of evapotranspiration the most at this scale.
- The type of aggregation of soil and plant resistances suitable for calculating the effective resistances in the patch varies depending on the type of resistance (i.e., surface or aerodynamic), and the type of vegetation predominant in the patch, which determines the number of soil and plant resistances considered.
- For a semi-arid area like the one we studied, the aggregation of soil, plant and

atmospheric aerodynamic resistances for calculating the effective aerodynamic resistance gives better results than calculating it directly from the wind speed at reference height and the parameter kB^{-1}.

Acknowledgements. This work received financial support from several different research projects: the PROBASE (ref.: CGL2006-11619/HID) and CANOA (ref.: CGL2004-04919-C02-01/HID) projects funded by the Spanish Ministry of Education and Science; and the BACAEMA ("Balance de carbono y de agua en ecosistemas de matorral mediterrneo en Andalucía: Efecto del cambio climático", RNM-332) and CAMBIO ("Efectos del cambio global sobre la biodiversidad y el funcionamiento ecosistémico mediante la identificación de áreas sensibles y de referencia en el SE ibérico", RNM 1280) projects funded by the regional government Junta de Andaluca. The first author enjoyed a pre-doctoral grant from the Spanish Ministry of Science and Technology. The authors would like to thank A. Durán Sánchez and M. Guerrero Berenguel for their invaluable help in the field work, and D. Fuldauer for correcting and improving the English of the text.

References

Alados-Arboledas, L., Olmo, F. J., Puigdefábregas, J., Domingo, F., and Villagarcía, L.: Using Infrared Remote Sensing for the Estimation of Sensible Heat Flux over Sparse Vegetation in Southeastern Spain. 1-2. Lagos. 2° Asamblea Hispano Portuguesa de Geodesia y Geofísica, 2000.

Baldocchi, D. D., Luxmoore, J., and Hatfield, J. L.: Discerning the forest from the trees: an essay on scaling canopy stomatal conductance, Agric. Forest Meteorol., 54, 197–226, 1991.

Blyth, E. M., Dolman, A. J., and Wood, N.: Effective resistance to sensible- and latent-heat flux in heterogeneous terrain, Q. J. R. Meteorol. Soc., 119, 423–442, 1993.

Blyth, E. M.: Using a simple SVAT scheme to describe the effect of scale on aggregation, Bound.-Layer Meteorol., 72, 267–285, 1995.

Blyth, E. M.: Representing heterogeneity at the southern super site with average surface paramenters, J. Hydrol., 188–189, 869–877, 1997.

Brenner, A. J. and Incoll, L. D.: The effect of clumpling and stomatal response on evaporation from sparsely vegetated shrublands, Agric. Forest Meteorol., 84, 187–205, 1997.

Brutsaert, W.: Heat and mass transfer to and from surfaces with dense vegetation or similar permeable roughness, Bound.-Layer Meteorol., 16, 365–388, 1979.
Cantón, Y., Solé-Benet, A., and Domingo, F.: Temporal and spatial patterns of soil moisture in semiarid badlands of SE Spain, J. Hydrol., 285, 199–214, 2004.
Chehbouni, A., Lo Seen, D., Njoku, E. G., Lhomme, J. P., Monteny, B. A., and Kerr, Y. H.: Estimation of sensible heat flux over sparsely vegetated surfaces, J. Hydrol., 188–189, 855–868, 1997.
Chehbouni, A., Watts, C., Kerr, Y. H., Dedieu, G., Rodriguez, J. C., Santiago, F., Cayrol, P., Boulet, G., and Goodrich, D. C.: Methods to aggregate turbulent fluxes over heterogeneous surfaces: application to SALSA data ser in Mexico, Agric. Forest Meteorol., 105, 133–144, 2000.
Choudhoury, B. J. and Monteith, J. L.: A four-layer model for the heat budget of homogeneous land surfaces, Q. J. R. Meteorol. Soc., 114, 373–398, 1988.
Daamen, C. C., Simmonds, L. P., Wallace, J. S., Laryea, K. B., and Sivakumar, M. V. K.: Use of microlysimeters to measure evaporation from sandy soils, Agric. Forest Meteorol., 65, 159–173, 1993.
Dolman, A. J.: A note on areally-averaged evaporation and the value of the effective surface conductance, J. Hydrol., 138, 583–589, 1992.
Dolman, A. J.: A multiple-source land surface energy balance model for use in general circulation models, Agric. Forest Meteorol., 65, 21–45, 1993.
Dolman, A. J. and Blyth, E. M.: Patch scale aggregation of heterogeneous land surface cover for mesoscale meteorological models, J. Hydrol., 190, 252–268, 1997.
Domingo, F., Van Gardingen, P. R., and Brenner, A. J.: Leaf boundary layer conductance of two native species in southeast Spain, Agric. Forest Meteorol., 81, 179–199, 1996.
Domingo, F., Villagarcía, L., Brenner, A. J., and Puigdefábregas, J.: Evapotranspiration model for semi-arid shrub-lands tested against data from SE Spain, Agric. Forest Meteorol., 95, 67–84, 1999.
Domingo, F., Villagarcía, L., Brenner, A. J., and Puigdefábregas, J.: Measuring and modelling the radiation balance of a heterogeneous shrubland, Plant Cell Environ., 23, 27–38, 2000.
Domingo, F., Villagarcía, L. Boer, M. M., Alados-Arboledas, L., and Puigdefábregas, J.: Evaluating the long-term water balance of arid zone stream bed vegetation using evapotranspiration modelling and hillslope runoff measurements, J. Hydrol., 243, 17–30, 2001.
Fiedler, F. and Panofsky, H.: The geostrophic drag coefficient and the effective roughness

length, Q. J. R. Meteorol. Soc., 98, 213–220, 1976.
Fuchs, M.: Heat flux, in: Methods of Soil Analysis Part I. Physical and Mineralogical Methods, Vol.2, edited by: Klute, A., American Society of Agronomy, Madison, WI, 957–968, 1986.
Garrat, J. R.: Transfer characteristics for a heterogeneous surface of large aerodynamic roughness, Q. J. R. Meteorol. Soc., 104, 491–502, 1978.
Gutiérrez, L.: Estructura y Productividad de la vegetación de estepa mediterránea semiárida en relación con la variabilidad climática: el sistema de ladera en Rambla Honda (Almería). PhD Thesis, Universidad de Almería. Almería, Spain, 2000.
Haase, P., Pugnaire, F. I., Fernández, E. M. Puigdefábregas, J., Clark, S. C., and Incoll, L. D.: An investigation of rooting depth of the semi-arid shrub *Retama sphaerocarpa* (L.) Boiss. by labelling of ground water with a chemical tracer, J. Hydrol., 177, 23–31, 1996.
Jones, H. G.: Plants and microclimate: a quantitative approach to environmental plant physiology, Cambridge University Press, London, 1992.
Kowalski, A. S., Anthoni, P. M., Vong, R. J., Delany, A. C., and Maclean, G. D.: Deployment and Evaluation of a System for Ground-Based Measurement of Cloud Liquid Water Turbulent Fluxes, J. Atmos. Oceanic Technol., 14(3), 468–479, 1997.
Kustas, W. P., Choudhury, B. J., Moran, M. S., Reginato, R. J., Jackson, R. D., Gay, L. W., and Weaver, H. L.: Determination of sensible heat flux over sparse canopy using thermal infrared data, Agric. Forest Meteorol., 44, 197–216, 1989.
Mahrt, L.: Surface Heterogeneity and Vertical Structure of the Boundary Layer, Bound.-Layer Meteorol., 96, 33–62, 2000.
Massman, W. J.: A surface energy balance method for partitioning evapotranspiration data into plant and soil components for a surface with partial canopy cover, Water Resour. Res., 28, 1723–1732, 1992.
McInnes, K. J., Heilman, J. L., and Lascano, R. J.: Aerodynamic conductances at the soil surface in a vineyard, Agric. Forest Meteorol., 79, 29–37, 1996.
McInnes, K. J., Heilman, J. L., and Savage, M. J.: Aerodynamic conductances along a bare ridge-furrow tilled soil surface, Agric. Forest Meteorol., 68, 119–131, 1994.
McNaughton, K. G.: Effective stomatal and boundary-layer resistance of heterogeneous surfaces, Plant Cell Environ., 17, 1061–1068, 1994.
Mölder, M. and Lindroth, A.: Dependence of kB^{-1} factor on roughness Reynolds number for barley and pasture, Agric. Forest Meteorol., 106, 147–152, 2001.
Monteith, J. L.: Evaporation and Environment, Symposia of the Society of Experimental Biol-

ogy, 19, 205–234, 1965.
Noilhan, J., Lacarrère, P., Dolman, A. J., and Blyth, E.M.: Defining area-average parameters in meteorological models for land surfaces with mesoscale heterogeneity, J. Hydrol., 190, 302–316, 1997.
Puigdefábregas, J., Alonso, J. M., Delgado, L., Domingo, F., Cueto, M., Gutiérrez, L., Lázaro, R., Nicolau, J. M., Sánchez, G., Solé, A., and Vidal, S.: The Rambla Honda field site: interactions of soil and vegetation along a catena in semi-arid Spain, in: Mediterranean desertification and land use, edited by: Brandt, J. and Thornes, J. B., John Wiley & Sons, Ltd. Chischester, UK. 137-168, 1996.
Puigdefábregas, J. and Sanchez, G.: Geomorphological implications of vegetation patchiness on semi- arid slopes, Adv. Hill. Proc., 2, 1027–1060, 1996.
Puigdefábregas, J., Del Barrio, G., Boer, M. M., Gutiérrez, L., and Solé, A.: Differential responses of hillslope and channel elements to rainfall events in a semi-arid area, Geomorph., 23, 337–351, 1998.
Puigdefábregas, J., Solé, A., Gutiérrez, L., Del Barrio, G., and Boer, M. M.: Scales and processes of water and sediment redistribution in drylands: results from the Rambla Honda field site in Shoutheast Spain, Earth-Science Reviews., 48, 39–70, 1999.
Qualls, R. J. and Brutsaert, W.: The effect of vegetation density on the parameterization of scalar roughness to estimate spatially distributed sensible heat fluxes, Water Resour. Res., 32(3), 645–652, 1995.
Shuttleworth,W. J.: Hydrological models, regional evaporation and remote sensing: let's start simple and maintain perspective, in: Land Surface Processes in Hydrology: Trials and Tribulations of Modeling and Measuring, edited by: Sorooshian, S., Grupta, H. V., and Rodda, J., Springer. Berlin, Heidelberg, 1997.
Shuttleworth, W. J. and Gurney, R. J.: The theoretical relationships between foliage temperature and canopy resistance in sparse crops. Q. J. R. Meteorol. Soc., 116, 497–519, 1990.
Shuttleworth, W. J. and Wallace, J. S.: Evaporation from sparse crops, an energy combination theory, Q. J. R. Meteorol. Soc., 3, 839–855, 1985.
Tanner, B. D., Swiatek, E., and Green, J. P.: Density fluctuations and use of the krypton hygrometer in surface flux measurements, in: Proc. Management of Irrigation and Drainage Systems, ASCE, edited by: Allen, R. G. and Neale, C. M. U., Park City, UT, 105–112, 1993.
Van den Hurk, B. J. J. M. and McNaughton, K. G.: Implementation of near-field dispersion in a sample two-layer surface resistance model, J. Hydrol., 166, 293–311, 1995.

Verhoef, A. and Allen, S. J..: The relative importance of surface and aeordynamic resistances in a multi-source energy-CO_2 model, Phys. Chem. Earth, 23, 459–463, 1998.
Verhoef, A. and Allen, S. J.: A SVAT scheme describing energy and CO2 fluxes for multi-component vegetation: calibration and test for a Sahelian savannah, Ecol. Modell., 127, 245–267, 2000.
Verma, S. B.: Aerodynamic Resistances to Transfers of Heat, Mass and Momentum, 177, 13–20, IAHS Publ., Vancouver, 1989.
Vidal, S.: A device for simultaneous measurement of soil moisture and electrical conductivity. (Patent n° 9401681), 1994.
Vidal, S., Domingo, F., Solé-Benet, A. and Puigdefábregas, J.: Desarrollo y calibración de un nuevo sensor de humedad de suelo, in: IV Simposio sobre el Agua en Andalucia, Almería, Spain, Vol I, 101–109, 1996.
Webb, E. K., Rearman, G. I., and Leuning, R.: Correction of flux measurements for density effects due to heat and water vapour transfer, Q. J. R. Meteorol. Soc., 106, 85–100, 1980.

Table 1. Equations relating soil surface resistances (r_s^s, r_s^{su} and r_s^{bs}) to soil moisture (θ) and soil aerodynamic resistances (r_a^s, r_a^{su} and r_a^{bs}) to wind speed at reference height (u_r), for the two patches studied.

	r_s^s	r_s^{su}	r_s^{bs}	r_a^s	r_a^{su}	r_a^{bs}
R. sphaerocarpa		$7.74\theta^{-1.95}$	$0.45\theta^{-3}$		$98.4u_r^{-0.17}$	$73.7u_r^{-0.19}$
Herbaceous	$0.14\theta^{-3.8}$			$98.6u_r^{-0.22}$		

Table 2. Equations relating the coefficients g_s^{max} and b_d to soil moisture (θ) obtained by Brenner and Incoll (1997) for *R. sphaerocarpa*; and equation relating surface leaf conductance (g_s^l) to water vapour pressure deficit (D_a) for herbaceous plants.

	g_s^{max}	b_d	g_s^l
R. sphaerocarpa	$-1.38\theta-0.1$	$3.25\theta+0.34$	
Herbaceous			$0.25D_a^{-0.8}$

Table 3. Reference height (z_r), vegetation height (h), leaf area index (L) and fractional vegetation cover (f), for each vegetation patch. All values in meters, except L (in m^2m^{-2}) and f (unitless).

	z_r	h	L	f
R. sphaerocarpa	4.4	2.26	0.81	0.17
Herbaceous	2.5	0.22		

Table 4. Average ±SD (standard deviation) of the Δr differences between the effective resistances considered. **(a)** *R. sphaerocarpa* patch, **(b)** Herbaceous patch.

(a)		$\boldsymbol{r_i}$			
	Δr (%)	$\langle r_a^e \rangle_s$	$r_{a_1}^e$	$r_{a_2}^e$	$\langle r_s^e \rangle_s$
$\boldsymbol{r_j}$	$\langle r_a^e \rangle_p$	61.8±5.3	53±11.8	77.4±5.7	
	$\langle r_a^e \rangle_s$		–28.4±43.5	38.4±20.9	
	$\langle \overline{r_a^e} \rangle$		12.4±27.7	57.9±13.3	
	$r_{a_1}^e$			52.0±0.0	
	$\langle r_s^e \rangle_p$				38.2±4.1

(b)		$\boldsymbol{r_i}$			
	Δr (%)	$\langle r_a^e \rangle_s$	$r_{a_1}^e$	$r_{a_2}^e$	$\langle r_s^e \rangle_s$
$\boldsymbol{r_j}$	$\langle r_a^e \rangle_p$	52.9±4.2	50.3±14.1	75.3±7.0	
	$\langle r_a^e \rangle_s$		–7.8±36.7	46.3±18.2	
	$\langle \overline{r_a^e} \rangle$		21.2±25.3	60.8±12.6	
	$r_{a_1}^e$			50.3±0.1	
	$\langle r_s^e \rangle_p$				81.9±10.4

HESSD
4, 243–286, 2007

EGU

Table 5. Parameters b, a and R^2 from the regressions between measured and estimated λE, shown in Fig. 7. The level of significance p of each parameter is marked: $^{**}p < 0.01$, $^{*}p < 0.05$ and ^{ns} not significant ($p > 0.05$).

	R. sphaerocarpa patch			Herbaceous patch		
	b	a	R^2	b	a	R^2
$\lambda E \left\langle r_s^e \right\rangle_p r_{a_1}^e$	0.78^{**}	0.08^{ns}	0.62^{**}	0.96^{**}	0.17^{ns}	0.67^{**}
$\lambda E \left\langle r_s^e \right\rangle_s r_{a_1}^e$	0.55^{*}	0.05^{ns}	0.43^{*}	0.70^{**}	-0.25^{ns}	0.48^{**}
$\lambda E \left\langle \overline{r_s^e} \right\rangle r_{a_1}^e$	0.64^{*}	0.06^{ns}	0.50^{*}	0.90^{**}	-0.27^{ns}	0.58^{**}
$\lambda E \left\langle r_s^e \right\rangle_p r_{a_2}^e$	0.99^{**}	0.11^{ns}	0.72^{**}	1.08^{**}	0.23^{ns}	0.59^{**}
$\lambda E \left\langle r_s^e \right\rangle_s r_{a_2}^e$	0.75^{*}	0.06^{ns}	0.50^{*}	0.96^{**}	-0.32^{ns}	0.55^{**}
$\lambda E \left\langle \overline{r_s^e} \right\rangle r_{a_2}^e$	0.86^{**}	0.08^{ns}	0.58^{**}	1.14^{**}	-0.30^{ns}	0.66^{**}

Table 6. Parameters b, a and R^2 from the regressions between measured and estimated λE, shown in Fig. 8. The level of significance p of each parameter is marked: $^{**}p < 0.01$, $^{*}p < 0.05$ and ^{ns} not significant ($p > 0.05$).

	R. sphaerocarpa patch			Herbaceous patch		
	b	a	R^2	b	a	R^2
$\lambda E \left\langle r_s^e \right\rangle_p \left\langle r_a^e \right\rangle_p$	0.58^{**}	0.09^{ns}	0.64^{**}	0.68^{**}	0.24^{ns}	0.59^{**}
$\lambda E \left\langle r_s^e \right\rangle_p \left\langle \overline{r_a^e} \right\rangle$	0.66^{**}	0.14^{ns}	0.71^{**}	0.73^{**}	0.29^{ns}	0.52^{**}
$\lambda E \left\langle r_s^e \right\rangle_p \left\langle r_a^e \right\rangle_s$	0.74^{**}	0.18^{ns}	0.77^{**}	0.76^{*}	0.33^{ns}	0.47^{*}
$\lambda E \left\langle r_s^e \right\rangle_s \left\langle r_a^e \right\rangle_p$	0.39^{*}	0.05^{ns}	0.46^{*}	0.42^{*}	-0.13^{ns}	0.41^{*}
$\lambda E \left\langle r_s^e \right\rangle_s \left\langle \overline{r_a^e} \right\rangle$	0.45^{*}	0.10^{ns}	0.49^{*}	0.49^{*}	-0.13^{ns}	0.44^{*}
$\lambda E \left\langle r_s^e \right\rangle_s \left\langle r_a^e \right\rangle_s$	0.51^{*}	0.13^{ns}	0.54^{*}	0.55^{**}	-0.14^{ns}	0.47^{**}
$\lambda E \left\langle \overline{r_s^e} \right\rangle \left\langle r_a^e \right\rangle_p$	0.46^{*}	0.07^{ns}	0.53^{*}	0.58^{*}	-0.14^{ns}	0.51^{*}
$\lambda E \left\langle \overline{r_s^e} \right\rangle \left\langle \overline{r_a^e} \right\rangle$	0.54^{*}	0.11^{ns}	0.57^{*}	0.66^{**}	-0.14^{ns}	0.56^{**}
$\lambda E \left\langle \overline{r_s^e} \right\rangle \left\langle r_a^e \right\rangle_s$	0.60^{**}	0.15^{ns}	0.63^{**}	0.71^{**}	-0.13^{ns}	0.60^{**}

Table 7. Average (± SD) of differences $\Delta\lambda E$ between measured and estimated λE with the effective aggregated surface resistances and the effective aerodynamic resistances calculated with Eq. (4), for each patch. The averages were calculated with the real $\Delta\lambda E$ ($\Delta\lambda E$ %) and with the absolute values (ABS($\Delta\lambda E$ %)).

	R. sphaerocarpa patch		Herbaceous patch	
	$\Delta\lambda E$ %	ABS($\Delta\lambda E$ %)	$\Delta\lambda E$ %	ABS($\Delta\lambda E$ %)
$\lambda E \left\langle r_s^e \right\rangle_p r_{a_1}^e$	12±13	15±8	–20±16	21±15
$\lambda E \left\langle r_s^e \right\rangle_s r_{a_1}^e$	39±13	39±13	65±16	65±16
$\lambda E \left\langle \overline{r_s^e} \right\rangle r_{a_1}^e$	28±13	28±13	48±16	48±16
$\lambda E \left\langle r_s^e \right\rangle_p r_{a_2}^e$	13±13	13±13	–41±21	41±21
$\lambda E \left\langle r_s^e \right\rangle_s r_{a_2}^e$	16±16	19±11	50±19	50±19
$\lambda E \left\langle \overline{r_s^e} \right\rangle r_{a_2}^e$	5±15	13±8	29±18	30±16

Table 8. Average (± SD) of $\Delta\lambda E$ differences between measured and estimated λE with the different effective aggregated surface and aerodynamic resistances for each patch. The averages were calculated with the real $\Delta\lambda E$ ($\Delta\lambda E$ %) and with the absolute $\Delta\lambda E$ (ABS($\Delta\lambda E$ %)).

	R. sphaerocarpa patch		Herbaceous patch	
	$\Delta\lambda E$ %	ABS($\Delta\lambda E$) %	$\Delta\lambda E$ %	ABS($\Delta\lambda E$) %
$\lambda E \left\langle r_s^e \right\rangle_p \left\langle r_a^e \right\rangle_p$	31±10	31±10	–3±14	12±8
$\lambda E \left\langle r_s^e \right\rangle_p \left\langle \overline{r_a^e} \right\rangle$	15±10	16±8	–14±17	15±16
$\lambda E \left\langle r_s^e \right\rangle_p \left\langle r_a^e \right\rangle_s$	3±10	9±5	–23±20	23±20
$\lambda E \left\langle r_s^e \right\rangle_s \left\langle r_a^e \right\rangle_p$	54±9	54±9	75±11	75±11
$\lambda E \left\langle r_s^e \right\rangle_s \left\langle \overline{r_a^e} \right\rangle$	42±10	42±10	70±12	70±12
$\lambda E \left\langle r_s^e \right\rangle_s \left\langle r_a^e \right\rangle_s$	32±11	32±11	65±12	65±12
$\lambda E \left\langle \overline{r_s^e} \right\rangle \left\langle r_a^e \right\rangle_p$	45±10	45±10	62±12	62±12
$\lambda E \left\langle \overline{r_s^e} \right\rangle \left\langle \overline{r_a^e} \right\rangle$	32±10	32±10	54±12	54±12
$\lambda E \left\langle \overline{r_s^e} \right\rangle \left\langle r_a^e \right\rangle_s$	20±11	20±11	48±12	48±12

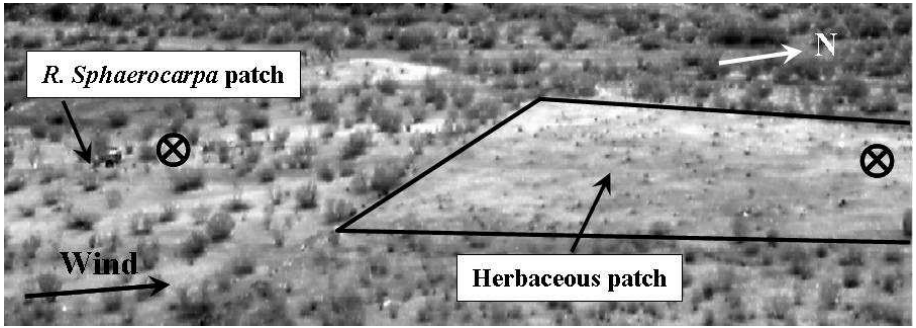

Fig. 1. View from the east of the two vegetation patches on the valley floor. The predominant wind speed direction and North are indicated. The location of the Eddy Covariance system in each patch is marked by a cross.

HESSD
4, 243–286, 2007

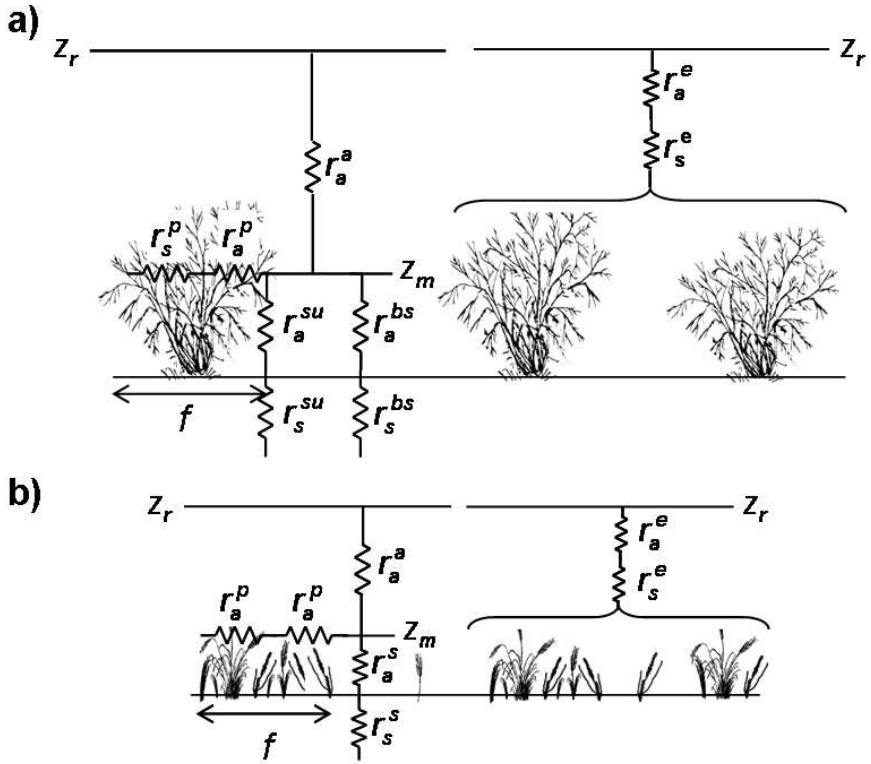

Fig. 2. Scheme showing the soil, plant and atmospheric resistances and the effective resistances (r^e) considered for each patch. **(a)** *R. sphaerocarpa* patch, **(b)** Herbaceous patch. See text for an explanation of symbols.

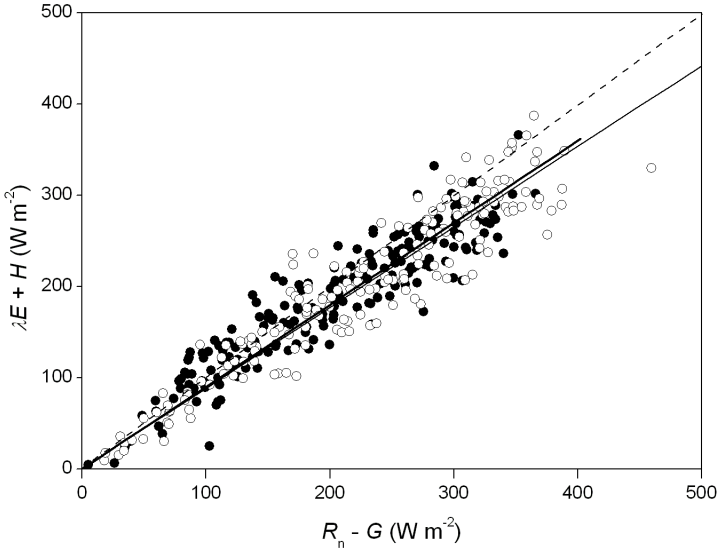

Fig. 3. Comparison of turbulent fluxes (λE + H) and measured available energy (R_n–G) in the two patches studied: ∘ *R. sphaerocarpa* patch (n=177); • herbaceous patch (n=197). The regression lines forced through the origin are shown (thin line: *R. sphaerocarpa* patch; thick line: herbaceous patch), and the 1:1 line (dashed line).

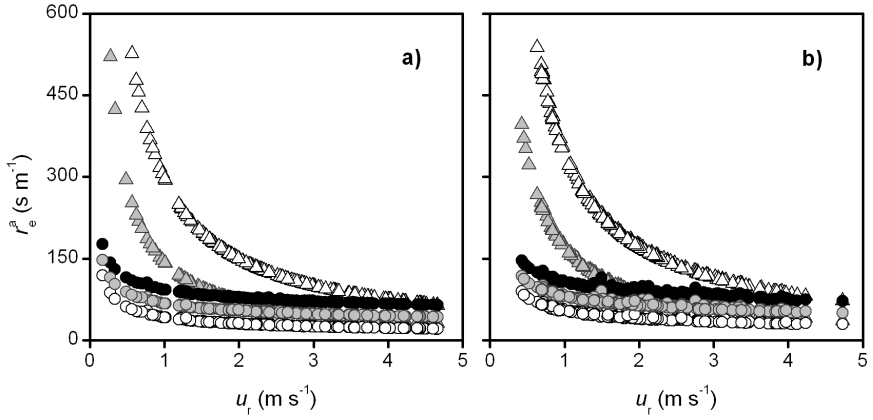

Fig. 4. Effective aerodynamic resistances (r_a^e) plotted against the wind speed at reference height (u_r): $r_{a_1}^e$ (△), $r_{a_2}^e$ (Δ), $\langle r_a^e \rangle_p$ (∘), $\langle r_a^e \rangle_s$ (•) and $\left\langle \overline{r_a^e} \right\rangle$ (◎). **(a)** *R. sphaerocarpa* patch; **(b)** Herbaceous patch.

HESSD
4, 243–286, 2007

EGU

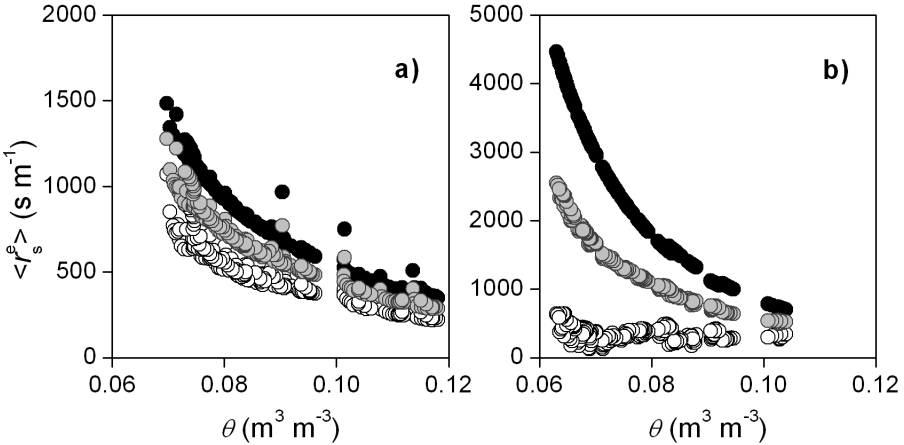

Fig. 5. Effective aggregated surface resistances ($\langle r_s^e \rangle$) plotted against the soil moisture (θ): $\langle r_s^e \rangle_p$ (∘), $\langle r_s^e \rangle_s$ (•) and $\left\langle \overline{r_s^e} \right\rangle$ (⊙). **(a)** *R. sphaerocarpa* patch; **(b)** Herbaceous patch.

HESSD
4, 243–286, 2007

EGU

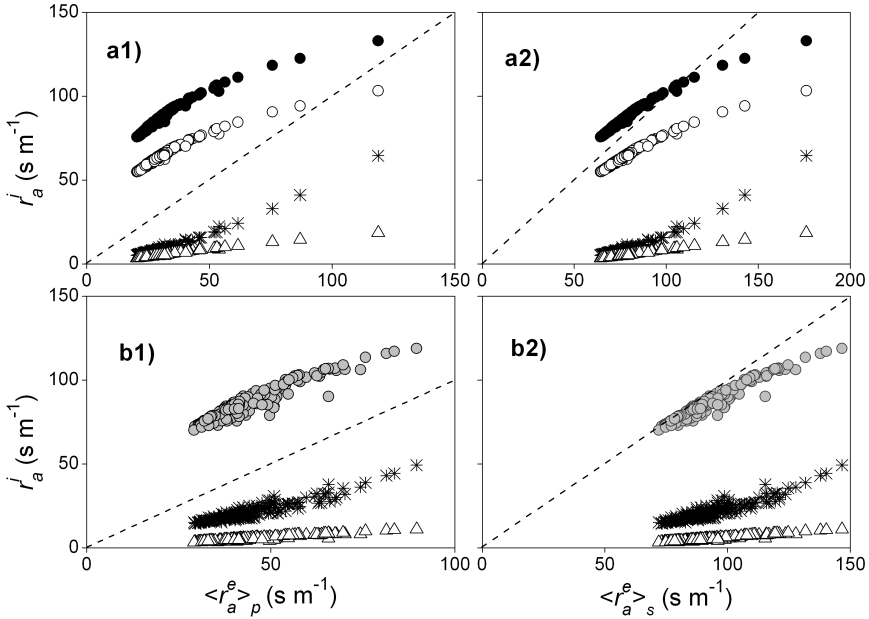

Fig. 6. Aerodynamic resistances of the sources (r_a^{su}:•; r_a^{bs}:∘; r_a^s:⊙; r_a^p: Δ) and r_a^a (∗) plotted against the effective aggregated aerodynamic resistances: $\langle r_a^e \rangle_p$ (**a1** and **b1**) and $\langle r_a^e \rangle_s$ (**a2** and **b2**). Plots (a1) and (a2) are for the *R. sphaerocarpa* patch, and plots (b1) and (b2) are for the herbaceous patch. The dashed line is the 1:1 line.

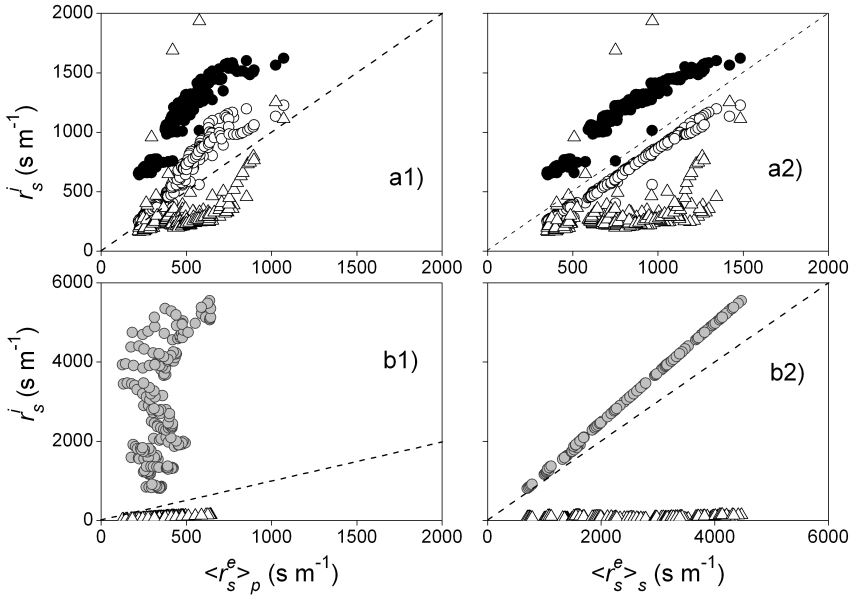

Fig. 7. Surface resistances of the sources (r_s^{su}: •; r_s^{bs}:∘; r_s^s: ○ and r_s^p: Δ) plotted against the effective aggregated surface resistances: $\langle r_s^e \rangle_p$ (**a1** and **b1**) and $\langle r_s^e \rangle_s$ (**a2** and **b2**). Plots (a1) and (a2) are for the *R. sphaerocarpa* patch, and plots (b1) and (b2) for the herbaceous patch. The dashed line is the 1:1 line.

HESSD
4, 243–286, 2007

EGU

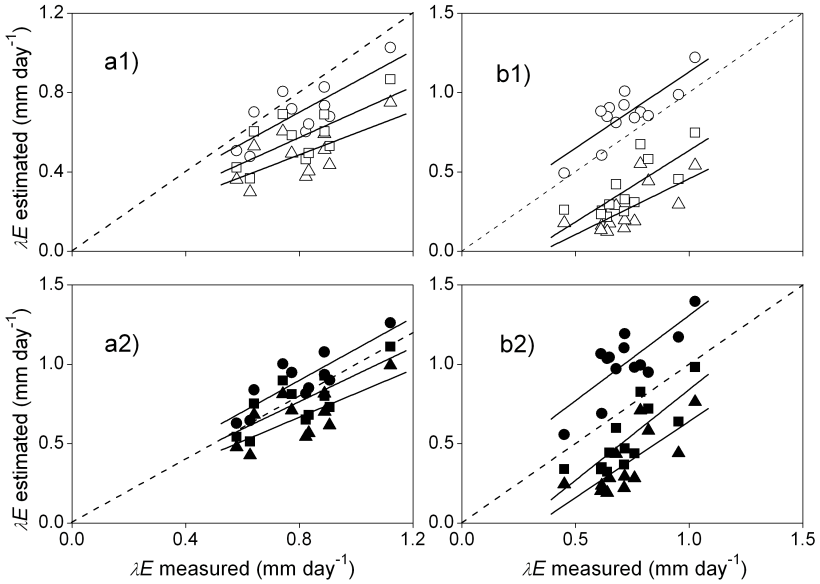

Fig. 8. Regressions between estimated and measured λE for the *R. sphaerocarpa* patch (**a1** and **a2**), and the herbaceous patch (**b1** and **b2**). λE was estimated using different combinations of effective surface and aerodynamic resistances: $\langle r_s^e \rangle_p$ and $r_{a_1}^e$ (∘); $\langle r_s^e \rangle_p$ and $r_{a_2}^e$ (•); $\left\langle \overline{r_s^e} \right\rangle$ and $r_{a_1}^e$ (□); $\left\langle \overline{r_s^e} \right\rangle$ and $r_{a_2}^e$ (■); $\langle r_s^e \rangle_s$ and $r_{a_1}^e$ (Δ); $\langle r_s^e \rangle_s$ and $r_{a_2}^e$ (▲). The regression lines (solid lines) and 1:1 line (dashed line) are shown.

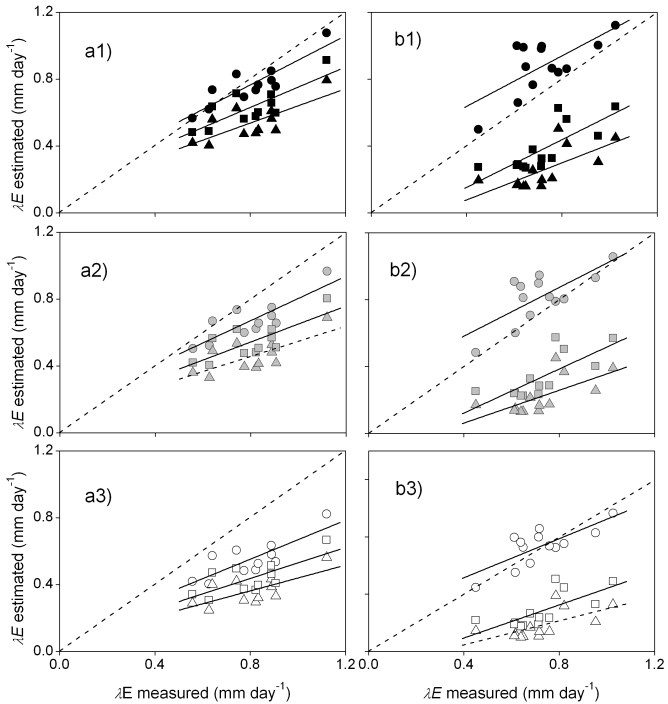

Fig. 9. Regressions between estimated and measured λE for the *R. sphaerocarpa* patch (Figs. **a1**, **a2**, and **a3**) and the herbaceous patch (Figs. **b1**, **b2**, and **b3**). λE was estimated using different combinations of effective surface and aerodynamic resistances: $\langle r_s^e \rangle_p$ and $\langle r_a^e \rangle_s$(•); $\langle r_s^e \rangle_p$ and $\left\langle \overline{r_a^e} \right\rangle$ (◦); $\langle r_s^e \rangle_p$ and $\langle r_a^e \rangle_p$ (◦); $\left\langle \overline{r_s^e} \right\rangle$ and $\langle r_a^e \rangle_s$(■); $\left\langle \overline{r_s^e} \right\rangle$ and $\left\langle \overline{r_a^e} \right\rangle$ (▫); $\left\langle \overline{r_s^e} \right\rangle$ and $\langle r_a^e \rangle_p$(□); $\langle r_s^e \rangle_s$ and $\langle r_a^e \rangle_s$(▲); $\langle r_s^e \rangle_s$ and $\left\langle \overline{r_a^e} \right\rangle$ (△);$\langle r_s^e \rangle_s$ and $\langle r_a^e \rangle_p$ (Δ). The regression lines are shown (solid lines) as well as the 1:1 line (dashed line).